# Enantioselectivity in Metabolism and Toxicity of 6PPD-Quinone in Salmonids

Rui Li[1,2], Holly Barrett[1], Pranav Nair[1], Minghua Wang[2], Linna Xie[1,3*], Hui Peng[1,4*]

[1] Department of Chemistry, University of Toronto, Toronto, Ontario M5S 3H6, Canada

[2] Department of Pesticide Science, College of Plant Protection, Nanjing Agricultural University, State & Local Joint Engineering Research Center of Green Pesticide Invention and Application, Nanjing, 210095, China

[3] China CDC Key Laboratory of Environment and Population Health, National Institute of Environmental Health, Chinese Center for Disease Control and Prevention, Beijing, 100021, China

[4] School of the Environment, University of Toronto, Toronto, Ontario M5S 3H6, Canada

[*] **Corresponding author: Linna Xie**, e-mail: linna.xie@utoronto.ca; **Hui Peng**, e-mail: hui.peng@utoronto.ca

## Abstract

The toxicity of *N*-(1,3-dimethylbutyl)-*N'*-phenyl-*p*-phenylenediamine quinone (6PPD-Q) in salmonids has been found to be sensitive to even minor structural changes on its alkyl side chain. Inspired by this, we herein isolated the enantiomers of 6PPD-Q and tested their *in vitro* metabolism in liver S9 of rainbow trout (*O. mykiss*), along with their toxicity in a coho salmon (*O. kisutch*) embryo (CSE-119) cell line. (*R*)-6PPD-Q was found to be rapidly metabolized in rainbow trout liver S9 with a half-life ($t_{1/2}$) of 12.3 minutes, which was 2.92 times faster than that of (*S*)-6PPD-Q. This was further evidenced by the preferential formation of an (*R*)-aryl-OH-6PPD-Q metabolite. Supporting this, enantioselective accumulation of (*S*)-6PPD-Q was found in rainbow trout *in vivo*. To further distinguish between kinetics and intrinsic toxicity, we tested the toxicity of 6PPD-Q enantiomers in the CSE-119 cell line with minimal metabolism of 6PPD-Q. (*R*)-6PPD-Q was found to strongly induce cytotoxicity in CSE-119 cells with an $EC_{50}$ of 17.7 μg/L, which was 3.94 times stronger than that of (*S*)-6PPD-Q. In summary, this study reported the enantioselectivity in both the toxicity and metabolism of 6PPD-Q, demonstrating that its toxicity should be mediated by specific protein binding.



**Keywords:** 6PPD-Q; Enantioselective metabolism; Enantioselective toxicity; Rainbow trout; Coho salmon


**Synopsis:** The metabolism and toxicity of 6PPD-Q in salmonids is enantioselective.

## Introduction

N-(1,3-dimethylbutyl)-*N'*-phenyl-*p*-phenylenediamine (6PPD) is an additive commonly used in tires to prevent their oxidative degradation, with 50 to 100 million tons utilized annually in the United States alone.[1-3] During its life cycle, 6PPD can be oxidized to *N*-(1,3-dimethylbutyl)-*N'*-phenyl-*p*-phenylenediamine-quinone (6PPD-Q),[4-6] which exerts extreme aquatic toxicity in coho salmon (*O. kisutch*) with a median lethal concentration ($LC_{50}$) of 95 ng/L.[7, 8] Interestingly, large interspecies variation was observed for the toxicity of 6PPD-Q even among species belonging to the *Salmonidae* family. For instance, 6PPD-Q was also found to be toxic to rainbow trout (*O. mykiss*) but not to the closely-related arctic char (*S. alpinus*);[9-11] however, the toxicity mechanism remains unknown. An in-depth exploration of the structure-related toxicity of 6PPD-Q is not only important to identify a safe replacement antioxidant for 6PPD but is also critical for understanding its toxicity mechanism.

Recent studies from our group discovered that even minor structural modifications to the alkyl side chain of 6PPD-Q can completely abolish its toxicity.[12, 13] Considering the presence of a chiral center on the second carbon ($C_2$) of its alkyl side chain, it is important to investigate the potential enantioselective toxicity of 6PPD-Q. Indeed, recent research from the Wang group has reported that (*S*)-6PPD-Q exhibited stronger toxicity than (*R*)-6PPD-Q in rainbow trout.[14, 15] The enantioselective toxicity of xenobiotics often arises from their intrinsic ability to selectively bind to specific protein targets. A well-known example is the greater teratogenicity of (*S*)-thalidomide compared to (*R*)-thalidomide in humans, which was later attributed to the selective binding of (*S*)-thalidomide to the cereblon (CRBN) protein.[16-18] Moreover, pharmacokinetic processes including absorption,

distribution, metabolism, and excretion (ADME) can be enantioselective and impact the downstream toxicity of chiral xenobiotics, with metabolism playing a particularly important role.[19-21] 6PPD-Q was found to be rapidly metabolized to its hydroxylated counterparts in rainbow trout, with these metabolites becoming predominate in fish tissues within 24 hours.[11-13] Interestingly, distinct from other PPD-Q analogues, 6PPD-Q is regioselectively hydroxylated on the $C_4$ tertiary carbon on its alkyl side chain to form the unique $C_4$-alkyl-OH-6PPD-Q metabolite.[12, 13, 22] The $C_4$-alkyl-OH-6PPD-Q metabolite was confirmed to be nontoxic, serving as a potential detoxification pathway for 6PPD-Q.[22] The potential contribution for this unique metabolite to the enantioselective toxicity of 6PPD-Q is worthy of further inquiry. However, distinguishing between the confounding factors of metabolism and intrinsic toxicity using *in vivo* testing alone is challenging. It remains unclear whether the enantioselective toxicity of (*S*)-6PPD-Q is driven by its metabolism or intrinsic toxicity.

In this study, we aimed to systematically investigate the enantioselectivity of 6PPD-Q in terms of both its metabolism and toxicity. To achieve this, we 1) purified 6PPD-Q enantiomers using preparative high performance liquid chromatography (prep-HPLC); 2) investigated the enantioselective metabolism of 6PPD-Q using liver S9 of rainbow trout; 3) assessed the intrinsic toxicity of 6PPD-Q enantiomers using a coho salmon embryonic (CSE-119) cell line where the contributions of metabolism to enantioselective toxicity can be mitigated. Unexpectedly, we discovered that the $C_2$ chiral carbon on the side alkyl chain influences both the metabolism and intrinsic toxicity of 6PPD-Q.

## Materials and methods

**Chemicals and Reagents.** 6PPD-Q and $d_5$-6PPD-Q standards were purchased from Toronto Research Chemicals (Toronto, ON, Canada). Liquid chromatography-mass spectrometry (LC-MS) grade acetonitrile and formic acid were purchased from Thermo Fisher Scientific (Waltham, MA, United States). Reagents and culture media used for the coho salmon cells, including Gibco fetal bovine serum, Leibovitz's (1X) (L-15 Medium), penicillin-streptomycin (10,000 U/mL), and 0.25% trypsin-ethylenediaminetetraacetic acid (EDTA; 1X) were purchased from Thermo Fisher Scientific (Waltham, MA, USA). Nicotinamide adenine dinucleotide phosphate (NADPH) tetrasodium salt (purity > 93%) and sodium phosphate dibasic ($Na_2HPO_4$) were purchased from Sigma Aldrich (Oakville, ON, Canada). Synthetic standards of two isomers of the alkyl-OH-6PPD-Q metabolites were prepared in-house, as is described in a previous procedure.[22]

**Separation and Isolation of 6PPD-Q enantiomers.** 6PPD-Q enantiomers were separated using a 1260 Infinity II high performance liquid chromatography (HPLC) system from Agilent Technologies (Santa Clara, CA, USA) equipped with a UV detector. The enantiomers were separated on a CHIRALPAK IA (Amylose tris 3,5-dimethylphenylcarbamate, 250 × 4.6 mm) column purchased from Daicel Chiral Technologies (Chiral Technologies Europe). The mobile phases consisted of 0.1% formic acid in water (20%) and 0.1% formic acid in acetonitrile (80%). The flow rate was 0.8 mL/min, and the injection volume was 100 µL. Dual-wavelength signals were monitored at 290 nm and 350 nm. Fractions were collected using a fraction collector at 30-second intervals from 10 to 16 minutes, and then the composition of each fraction was analyzed

using HPLC. The fractions of the same enantiomer were combined and further dried using nitrogen evaporation.

Analysis of 6PPD-Q enantiomers and metabolites were conducted using a Q Exactive Orbitrap high resolution mass spectrometer (HRMS) coupled with a Vanquish ultra-high performance liquid chromatography (UPLC) system from Thermo Fisher Scientific, USA equipped with a CHIRALPAK IA column. The column room temperature was set at 40°C. The mobile phases comprised 0.1% formic acid in water (A) and 0.1% formic acid in acetonitrile (B) at an isocratic flow with a ratio of 30% and 70%, and a flow rate of 1 mL/min. The scanning procedure included a full $MS^1$ scan, followed by successive data-independent acquisition (DIA) $MS^2$ scans. The full MS covered a *m/z* range of 200 to 700 at a resolution (R) of 70,000, with an AGC target of $1e^6$ in 60 ms. For positive mode, DIA $MS^2$ scans ranged from *m/z* = 200 to 400, with an isolation window of 10 *m/z*. Additional parameters included a resolution (R) of 17,500, an AGC target of 200,000 ions, and a maximum ionization time of 100 ms. Specific parameters from the tune file were: spray voltage of 3.25 kV, sheath gas flow rate of 30 L/hr, auxiliary gas flow rate of 7 L/hr, and capillary temperature of 300°C.

**Determination of absolute configurations using electronic circular dichroism (ECD).** ECD spectra were obtained using a JASCO J-1500 CD Spectrometer (JASCO Corp., Tokyo, Japan) at room temperature. The enantiomers of 6PPD-Q were dissolved in acetonitrile with a final concentration of 10 mg/L and placed in a quartz cell with a path length of 0.1 cm. Spectra were collected over a wavelength range of 225 – 380 nm, with a scan speed of 50 nm $min^{-1}$ and an average of five scans. Gaussian 09 W software was used

to acquire the calculated ECD spectra of 6PPD-Q enantiomers. Firstly, the molecular mechanics field (MM2) was used to optimize the 3D structures of (*R*)- and (*S*)-6PPD-Q. Then the geometric optimization and frequency calculations were conducted to get the most stable conformations of two enantiomers based on the B3LYP function of the 6-311+G (2d, p) basis set. Finally, the absolute configurations of the 6PPD-Q enantiomers were confirmed by comparing the calculated and experimental ECD spectra.

**Rainbow trout and arctic char liver S9 preparation.** The preparation of S9 from liver of rainbow trout or arctic char was reported in our previous study.[22] Briefly, the livers of rainbow trout and arctic char were rinsed with 1 mL of ice-cold phosphate buffer (0.08 M sodium phosphate, 0.02 M potassium phosphate, pH 7.4). After discarding the PBS, 0.2 g of tissue was finely minced with scissors into a 2 mL microcentrifuge tube. Then, 800 µL of phosphate buffer was added, and the tissue was homogenized using a Fisher Scientific Powergen 125 (FTH-115) blade-type homogenizer (Waltham, MA, USA). Following centrifugation at 9,000 *g* for 15 minutes at 4°C, the resulting supernatant (S9 fraction) was transferred to a new 1.5 mL Eppendorf tube. Total protein concentration was determined using a Bradford protein assay, and the supernatant (S9 fraction) was stored at -80°C. All steps were performed on ice, and equipment was cleaned with water and acetone before use.

***In vitro* metabolism.** *In vitro* metabolism experiments were conducted using a similar protocol reported in previous studies.[22] In a 2 mL centrifuge tube, 150 µg/L of (*rac*)-6PPD-Q was incubated with 1.0 mg/mL of rainbow trout/arctic char liver S9 in 47 µL of sodium phosphate buffer (50 mM, pH 8). The reaction was initiated by adding 3 µL of NADPH

(10.5 mM) to the above solution. Incubation proceeded at 20°C for 0, 10, 20, 40, 60, 90, 120, and 180 minutes, respectively. Reactions were quenched by transferring 40 μL of mixtures to 120 μL of ice-cold acetonitrile with 0.1 mg/L of $d_5$-6PPD-Q in a new tube, followed by vortex for 20 minutes and ultra-sonication for 15 minutes. Samples were centrifuged at 10,000 *g* for 10 minutes, and the supernatant was collected for analysis. For the negative controls, the procedures were the same as the above experiment, except that liver S9 was heat-deactivated at 95°C for 10 minutes. In blank controls, (*rac*)-6PPD-Q was replaced by the same volume of acetonitrile (< 1% *v/v*).

**Cell Viability Assay.** Cell viability of CSE-119 cells exposed to 6PPD-Q enantiomers was assessed using alamarBlue viability assay.[13, 24] The day before the exposure experiment, CSE-119 cells were seeded in 96-well plates at a density of 10,000 cells per well in 100 μL of culture media. After 24 hours of incubation, the culture media in the 96-well plate was replaced with exposure media containing 6PPD-Q enantiomers at 7 different concentrations (0.137 to 100 μg/L), each in 4 replicates. The acetonitrile concentration in the culture media was less than 0.2% (*v/v*), at which no significant toxicity was observed. Then cells were cultured for another 48 hours at 20°C, followed by addition of 10 μL of 0.30 mg/mL alamarBlue reagent per well and further incubation for 4 hours at 20°C. Fluorescence intensity was measured using a Tecan Infinite 200 Pro M Plex microplate reader (Tecan Life Sciences, Switzerland) at an excitation wavelength of 550 nm and an emission wavelength of 600 nm. Fluorescence values of each well were compared to solvent controls on the same plate to calculate cell viability.

**Assessing the metabolism of 6PPD-Q in CSE-119.** After culturing the cells in a petri dish

for 24 hours, the culture media was replaced with exposure media containing 6PPD-Q (10 μg/L), and the assessing of metabolism method was conducted according to a prior study.[23] For the control group, the same volume of fresh culture media, containing 0.1% acetonitrile, was added into the petri dish. Three replicates were included in both experimental and control groups. After 48 hours of incubation, the culture media was removed, and the cells were washed twice using 2 mL of phosphate-buffered saline (PBS). Following this, 1 mL of trypsin solution was added to detach the cells from the bottom of the petri dish. After the trypsin solution was discarded, 3 mL of PBS was added in order to collect the cells, which were then transferred to a 15 mL centrifuge tube, and centrifuged at 200 g for 10 minutes. The supernatant was discarded, and 1.2 mL of acetonitrile containing 6PPD-Q-$d_5$ was added to the pellet. The mixture was vortexed for 30 minutes and then sonicated for 30 minutes. Finally, the sample was centrifuged at 10,000 *g* for 10 minutes, and the supernatant was collected and evaporated under nitrogen until dryness. The extract was reconstituted in 100 μL of acetonitrile for LC-MS analysis.

**Quality Control and Quality Assurance.** Procedural blanks (acetonitrile only) were included in each batch of samples. During LC-MS analysis, an authentic standard of 6PPD-Q was injected after each group of 15 samples to check the stability of instrument. Acetonitrile was injected after each group of 8 samples to monitor potential carry-over. Strong linearity ($R^2 > 0.99$) was obtained for the external calibration curve of 6PPD-Q in the range of 6.25 to 100 μg/L. The 6PPD-Q-$d_5$ was used as the internal standard to correct potential loss of 6PPD-Q during extraction of liver S9 and CSE-119 cells. Due to the lack of standards, hydroxylated metabolites of 6PPD-Q except for $C_4$-OH-6PPD-Q were semi-quantified using 6PPD-Q. In the experiment of *in vitro* metabolism, the recoveries of (*R*)-

6PPD-Q and (*S*)-6PPD-Q were 104±5.4% and 99.5±8.2% in rainbow trout S9, and 114± 13.8% and 105 ± 7.0% in arctic char S9. The method detection limits (MDLs) were determined by the *y* intercept divided by the 99% confidence level of the slope of the calibration curve, and the detection limits of (*R*)-6PPD-Q and (*S*)-6PPD-Q for the incubation mixtures were 2.2 – 2.7 μg/L and 2.4 – 3.0 μg/L, respectively.

**Statistical analysis.** Statistical analyses were primarily conducted using GraphPad Prism (v10.1.2, GraphPad Software Inc., Boston, MA, USA). The enantioseparation was evaluated using resolution factor (Rs), as follows:

$$Rs = 2(t_{R2} - t_{R1})/(W_1 + W_2) \quad (1)$$

wherein $t_R$ and W represented the retention time and peak width of the enantiomer, respectively.

The first-order kinetics of the metabolism in liver S9 was fitted by the following equations:[25]

$$Ln(C_t/C_0)=-k\cdot t \quad (2)$$

$$t_{1/2}=ln2/k \quad (3)$$

wherein t, $C_t$, $C_0$, k, and $t_{1/2}$ were the incubation time, substrate concentrations at time t, initial concentration, first-order rate constant ($h^{-1}$), and half-life, respectively.

Enantiomer fraction (EF) was used to evaluate the enantioselective metabolism of 6PPD-Q enantiomers,[26] as follows:

$$EF=C_S/(C_R+C_S) \quad (4)$$

where $C_R$ and $C_S$ represented the concentrations of the *(R)*-enantiomer and *(S)*-enantiomer, respectively.

## Results and discussion

**Isolation and structure characterization of 6PPD-Q enantiomers.** Since the enantiomers of 6PPD-Q (Figure 1A) were not commercially available, we purified its enantiomers from a racemic mixture. The CHIRALPAK IA column was selected among various chiral columns as it achieved a baseline separation of 6PPD-Q enantiomers, wherein two peaks eluted at 11.09 minutes and 14.67 minutes, respectively (Figure 1B). The separation factor (3.49) was well above 1.5, demonstrating a complete separation of the two enantiomers. We then used the same CHIRALPAK IA column to purify enantiomers from the racemic mixture of 6PPD-Q. Approximately 1 mg of enantiomers were successfully obtained (Figure S1). The purity of each enantiomer was confirmed to exceed 98 % via LC-UV (Figure S2).

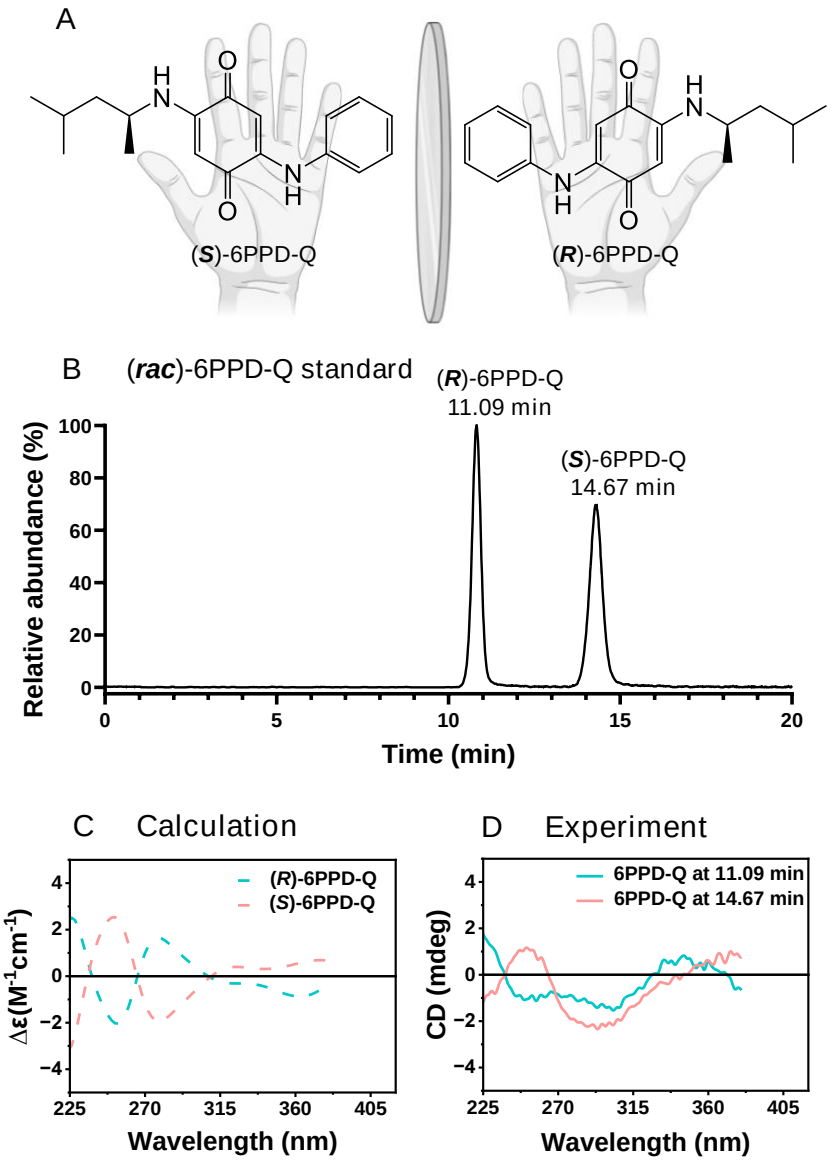


**Figure 1.** Isolation and absolute configuration of 6PPD-Q enantiomers. (A) Structures of (*R*)-6PPD-Q and (*S*)-6PPD-Q. (B) Chromatogram of 6PPD-Q enantiomers on the CHIRALPAK IA column. (C) The ECD spectra of 6PPD-Q enantiomers calculated by DFT. (D) Experimental ECD spectra of 6PPD-Q enantiomers.

We then employed ECD spectroscopy to determine the absolute configurations of two enantiomers, in combination with density functional theory (DFT) calculations. Figures 1C and 1D present the calculated and experimental ECD spectra, respectively. The

experimental ECD spectra for the two peaks at 11.09 minutes and 14.67 minutes align with the calculated spectra of (*R*)-6PPD-Q and (*S*)-6PPD-Q, in the two major absorbance regions (<270 and >350 nm) of 6PPD-Q.[27] The discrepancies between calculated and experimental spectrum at 290-350 nm might be attributed to the low absorbance in this region,[28] and the small Δε of 6PPD-Q. Therefore, the results demonstrated that (*R*)-6PPD-Q (RT=11.09 min) was eluted earlier from the CHIRALPAK IA column than (*S*)-6PPD-Q (RT=14.67 min), which was consistent with a previous study from Wang et al. using a similar chiral column.[14]

***In vitro* and *in vivo* enantioselective metabolism of 6PPD-Q in rainbow trout.** After isolating the 6PPD-Q enantiomers, we proceeded to assess their metabolism using liver S9 as an *in vitro* model. As shown in Figure 2A, >90 % of 6PPD-Q was rapidly depleted within 90 minutes after the incubation of (*rac*)-6PPD-Q with rainbow trout liver S9, while such depletion was not observed in the negative controls (heat deactivated S9). The metabolism of 6PPD-Q in rainbow trout liver S9 was much faster than other common pollutants under similar conditions, such as fenamidon, tembotrione and trifloxystrobin.[29] This aligned with previous *in vivo* studies showing that 6PPD-Q was rapidly metabolized in rainbow trout fish within 24 hours.[13]

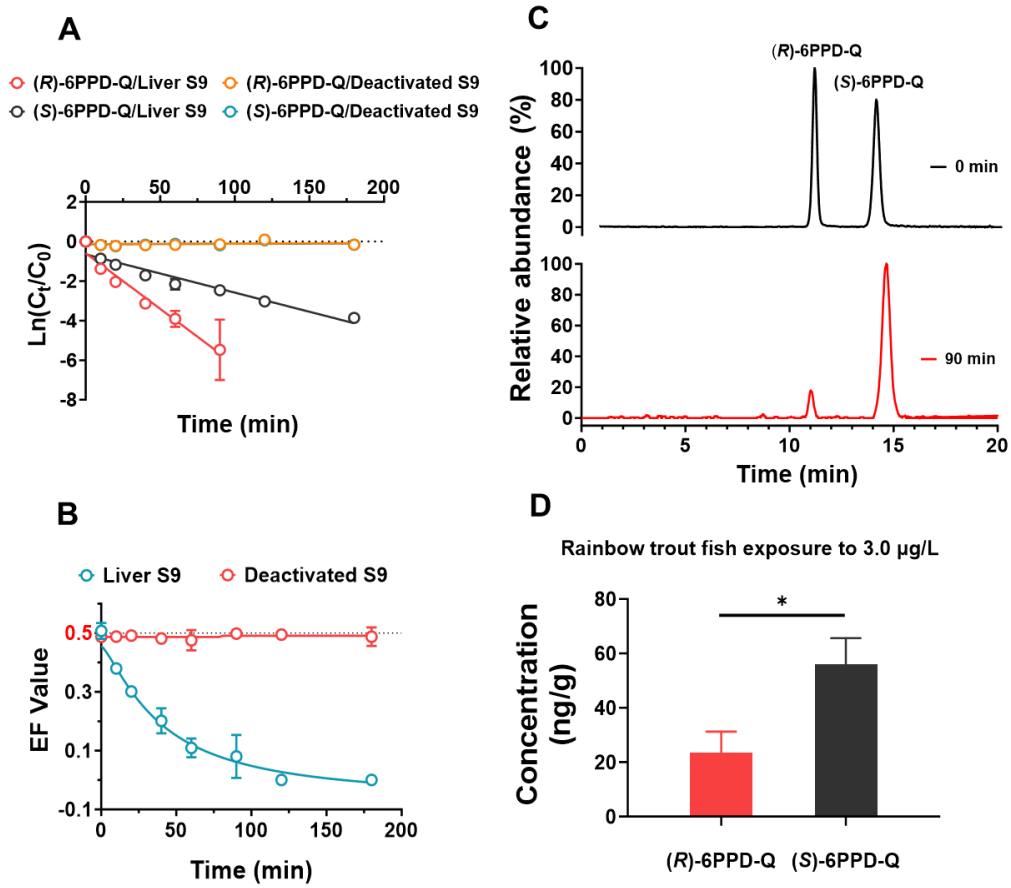


249

250 **Figure 2.** Metabolism of 6PPD-Q in rainbow trout. (A) Time-dependent metabolism of
251 6PPD-Q enantiomers in liver S9. (B) Time-dependent EF values of 6PPD-Q enantiomers
252 in liver S9. (C) The chromatograms of 6PPD-Q enantiomers after 0 (top panel) and 90 min
253 (bottom panel) of reactions with S9. (D) The concentrations of 6PPD-Q enantiomers in
254 rainbow trout whole-body tissue after exposure to 3 μg/L of (*rac*)-6PPD-Q. *denotes $p <$
255 0.05.

256 The rapid metabolism of (*R*)-6PPD-Q and (*S*)-6PPD-Q resulted in half-lives of 12.3 and
257 35.9 minutes, respectively (Figure 2A). This demonstrated that (*R*)-6PPD-Q was
258 metabolized in rainbow trout liver S9 at a rate of 2.92 times faster than that of (*S*)-6PPD-
259 Q. Correspondingly, the enantiomeric fraction (EF) value of (*R*)-6PPD-Q decreased from
260 0.51 ± 0.03 at 0 minutes to 0.08 ± 0.07 at 90 minutes ($p < 0.001$, Figure 2B). The
261 preferential metabolism of (*R*)-6PPD-Q was clearly observed by comparing the chiral

chromatograms of 6PPD-Q, wherein the two enantiomers initially displayed similar peak abundances, but (*S*)-6PPD-Q dominated after 90 minutes of incubation with liver S9 (Figure 2C). This is the first report of the enantioselective metabolism of 6PPD-Q, and was surprising given the small size of the methyl group on the $C_2$ chiral carbon.

To further confirm the potential enantioselective metabolism of 6PPD-Q *in vivo*, we analyzed the 6PPD-Q enantiomers present in rainbow trout tissue collected in our previous study, from fish that were exposed to 3.0 µg/L of (*rac*)-6PPD-Q for 96 hours.[12] This dose was chosen as it was close to the $LD_{50}$ (2.08 µg/L) of (*rac*)-6PPD-Q in rainbow trout.[12] As shown in Figure 2D, 2.38-fold stronger accumulation of (*S*)-6PPD-Q (56.0 ± 7.9 ng/g) relative to (*R*)-6PPD-Q (23.5 ± 6.3 ng/g, $p = 0.01$) was observed in fish tissues after exposure to 3.0 µg/L of (*rac*)-6PPD-Q for 96 hours. This finding aligns with *in vitro* liver S9 results, wherein (*R*)-6PPD-Q was metabolized more rapidly than (*S*)-6PPD-Q. Based on these *in vitro* and *in vivo* results, we concluded that the preferential metabolism of (*R*)-6PPD-Q led to its lower bioaccumulation in rainbow trout tissue. Recent studies from the Wang group reported that (*R*)-6PPD-Q exhibited 2.60 times weaker toxicity in rainbow trout,[14] which was comparable to its faster metabolism rate (2.92 times faster) and weaker accumulation (2.38 times) observed in the current study. Our recent study found that the hydroxylation metabolism of 6PPD-Q is a detoxification pathway,[22] thus, the enantioselective toxicity of 6PPD-Q in rainbow trout should be partially attributed to differential metabolism and detoxification of enantiomers.

**Enantioselective formation of hydroxylated metabolites in rainbow trout liver S9.** To further investigate the enantioselective metabolism pathways of 6PPD-Q, we employed high-resolution mass spectrometry based nontargeted analysis to identify metabolites in

rainbow trout liver S9. Consistent with our previous studies,[13] a total of five mono- and di-hydroxylated metabolites were detected from (*rac*)-6PPD-Q after incubation with rainbow trout liver S9 (see structures in Figure 3D). Specifically, four mono-hydroxylated 6PPD-Qs (*m/z* =315.1700, $C_{18}H_{22}N_2O_3$) were detected, at the retention times of 5.36 (I), 5.86 (II), 7.08 (III), and 7.33 (IV) minutes on the CHIRALPAK IA column, respectively (Figure 3A, S3A-3D). Using a chemical standard synthesized in our recent study,[22] metabolites III and IV were confirmed to be (*S*)- and (*R*)-$C_4$-OH-6PPD-Q, respectively (Figure S4A and Figure S5A). Among the five OH-6PPD-Qs, $C_4$-OH-6PPD-Q was of particular interest because it was previously shown to be selectively formed from 6PPD-Q, but not other PPD-Qs, despite their structural similarity.[12] The successful separation of $C_4$-OH-6PPD-Q enantiomers provided an opportunity to explore its formation mechanism. Similar to $C_4$-OH-6PPD-Q, the minor metabolite II was also assigned as an alkyl-OH-6PPD-Q, based on its diagnostic fragment of *m/z* 99.0808 (Figure S3B). We excluded the possibility of this metabolite being $C_3$-OH-6PPD-Q by using a synthesized chemical standard also prepared in-house alongside the $C_4$ standard, so it was likely $C_5$-OH-6PPD-Q. The metabolite I at 5.36 min was assigned as aryl-OH-6PPD-Q according to the diagnostic fragments of *m/z* 231.0766, *m/z* 257.0918 and *m/z* 273.1227 with hydroxyl group on the aryl ring (Figure S3A), but its enantiomers could not be separated on the CHIRALPAK IA column.

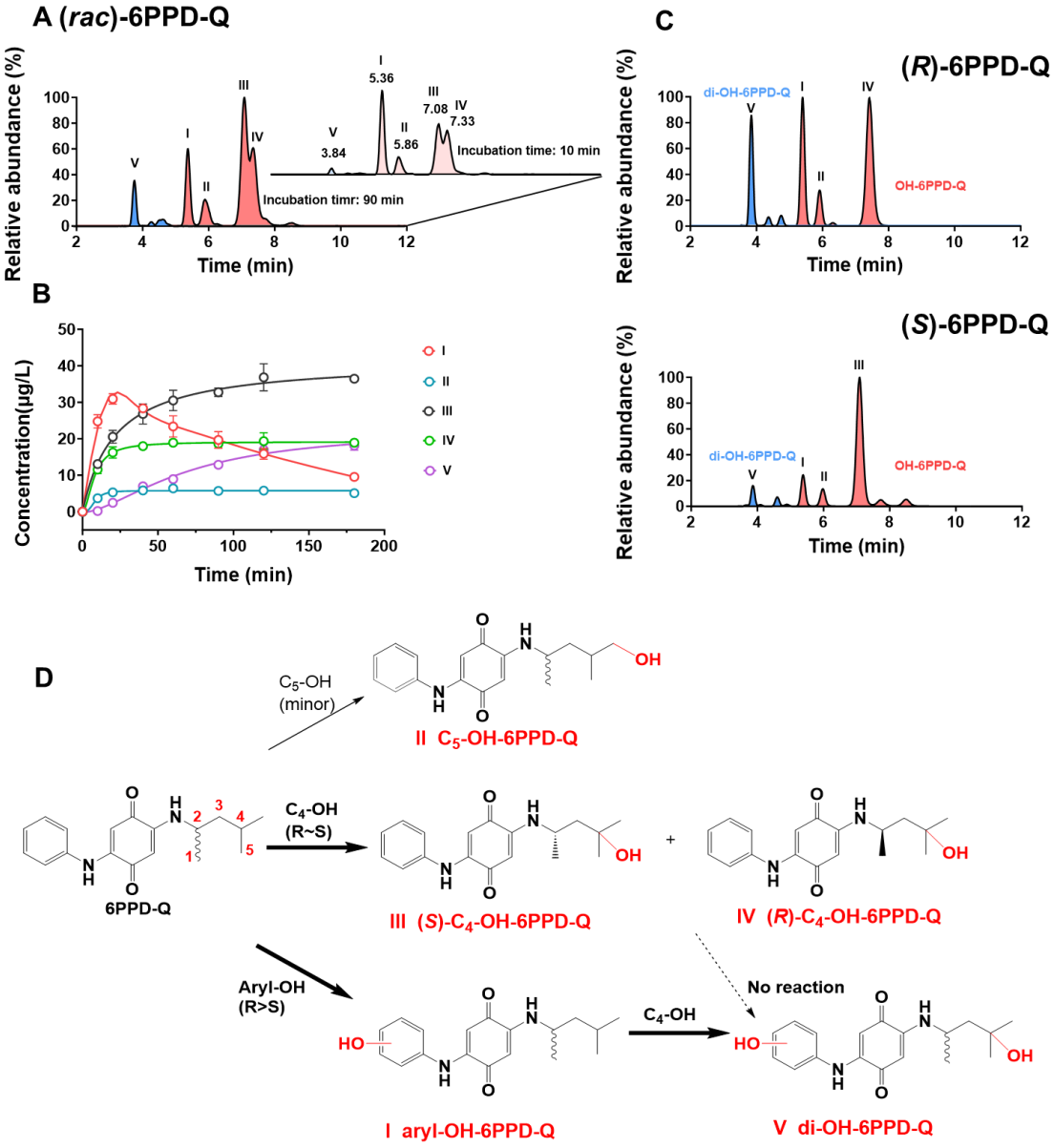


**Figure 3.** Hydroxylated metabolites of 6PPD-Q detected in liver S9 of rainbow trout. (A) A total of five hydroxylated metabolites of 6PPD-Q were detected in liver S9 after incubation with (*rac*)-6PPD-Q. (B) Time-dependent formation of hydroxylated metabolites in liver S9 of rainbow trout. (C) Chromatograms of mono- (red) and di-hydroxylated (blue) metabolites formed in liver S9 from (*R*)-6PPD-Q and (*S*)-6PPD-Q, respectively. (D) Proposed hydroxylation metabolism pathways of 6PPD-Q enantiomers. Note that the metabolism of 6PPD-Q to aryl-OH-6PPD-Q is enantioselective, and di-OH-6PPD-Q was primarily formed from aryl-OH-6PPD-Q.

In addition to the four mono-hydroxylated 6PPD-Qs, a di-hydroxylated 6PPD-Q metabolite (V) was also detected with *m/z* of 331.1653 (RT = 3.84 min, $C_{18}H_{22}N_2O_4$). Its $MS^2$ spectrum indicated hydroxyl groups on the aryl and alkyl side chains, separately (Figure S3E). By comparing its $MS^2$ spectrum with those of synthesized $C_3$-OH-6PPD-Q, $C_4$-OH-6PPD-Q, and the metabolite (V), the hydroxyl group on the alkyl side chain was very likely on $C_4$ (Figure S5). Collectively, we detected 5 hydroxylated 6PPD-Q metabolites in the liver S9 of rainbow trout, and successfully separated the enantiomers of the key $C_4$-alkyl-OH-6PPD-Q metabolite.

After incubating (*rac*)-6PPD-Q in the liver S9 of rainbow trout for 180 minutes, the total concentration (88.2 ± 0.28 μg/L, Figure 3B) of 5 hydroxylated metabolites explained the majority (58.8 ± 0.19%) of the 6PPD-Q loss from the initial amount (150 μg/L). We initially focused on $C_4$-OH-6PPD-Q, as it is the only metabolite with separable enantiomers. Both (*R*)- and (*S*)-$C_4$-OH-6PPD-Q enantiomers showed similar abundances during the first 10 minutes of incubation (Figure 3B, EF = 0.53 ± 0.01, $p$ = 0.16), demonstrating comparable rates of formation from 6PPD-Q. This findings suggested that the metabolism of 6PPD-Q to $C_4$-OH-6PPD-Q was not enantioselective. Interestingly, (*S*)-$C_4$-OH-6PPD-Q was continuously formed over time, while (*R*)-$C_4$-OH-6PPD-Q remained stable after 40 minutes. The faster formation of (*S*)-$C_4$-OH-6PPD-Q after 40 minutes didn't align with the more rapid depletion of (*R*)-6PPD-Q (*e.g.*, 4.33 ± 0.99 μg/L at 40 minutes) compared to (*S*)-6PPD-Q (*e.g.*, 17.1 ± 0.89 μg/L at 40 minutes), suggesting that other metabolic pathways should be primarily responsible for the enantioselective metabolism of 6PPD-Q.

**Enantioselective metabolism of 6PPD-Q was driven by the preferential formation of (*R*)-aryl-OH-6PPD-Q.** After excluding the $C_4$-OH-6PPD-Q pathway, we proceeded to test whether other pathways cause the enantioselective metabolism of 6PPD-Q. To test this, we separately incubated the enantiomers of 6PPD-Q with the liver S9 of rainbow trout, as most hydroxylated metabolites can not be separated on the chiral column. Interestingly, as shown in Figure 3C, distinct profiles of hydroxylated metabolites were formed from (*R*)- and (*S*)-6PPD-Q. Particularly, aryl-OH-6PPD-Q contributed to 39.3 ± 1.05% of total hydroxylated metabolites generated from (*R*)-6PPD-Q, which was significantly higher that from (*S*)-6PPD-Q (15.0 ± 0.19%, $p<0.001$). This clearly demonstrated the preferential metabolism of (*R*)-6PPD-Q to (*R*)-aryl-OH-6PPD-Q, a result that was not evident in the experiments with racemic 6PPD-Q. In addition, the preferential formation of (*R*)-aryl-OH-6PPD-Q well-explained the faster metabolism of (*R*)-6PPD-Q as mentioned above. Taking all the data into account, we concluded that enantioselective metabolism of 6PPD-Q should be primarily driven by the preferential formation of (*R*)-aryl-OH-6PPD-Q.

In addition to the faster formation of (*R*)-aryl-OH-6PPD-Q from (*R*)-6PPD-Q, a higher amount of di-OH-6PPD-Q was also produced from (*R*)-6PPD-Q (Figure 3C). Specifically, di-OH-6PPD-Q accounted for 2.87 ± 0.46% of total hydroxylated metabolites formed from (*R*)-6PPD-Q, which was significantly higher than that from (*S*)-6PPD-Q (0.74 ± 0.17%, $p<0.001$). The faster formation of di-OH-6PPD-Q and aryl-OH-6PPD-Q from (*R*)-6PPD-Q demonstrated that they share the same metabolic pathway. Supporting this, the formation of di-OH-6PPD-Q was rapid during the first 20 minutes of incubation with S9 but slowed down after 40 minutes (Figure 3B). This trend aligned with the decrease in the

concentrations of aryl-OH-6PPD-Q after 40 minutes, which further suggested that di-OH-6PPD-Q was likely formed from aryl-OH-6PPD-Q, rather than from $C_4$-OH-6PPD-Q. To further confirm this, we incubated synthesized $C_4$-OH-6PPD-Q with rainbow trout liver S9. As expected, $C_4$-OH-6PPD-Q was not significantly metabolized, and no formation of di-OH-6PPD-Q was observed after incubation with liver S9 for 60 minutes (Figure S6). This clearly demonstrated that di-OH-6PPD-Q should be primarily formed from aryl-OH-6PPD-Q.

In summary, 6PPD-Q was metabolized in rainbow trout through one minor and two major pathways. Of the two major pathways, the enantioselective metabolism of 6PPD-Q was primarily driven by the preferential formation of (*R*)-aryl-OH-6PPD-Q. Additionally, di-OH-6PPD-Q was primarily formed from aryl-OH-6PPD-Q rather than from $C_4$-OH-6PPD-Q (Figure 3D).

***In vitro* toxicity of 6PPD-Q enantiomers in a CSE-119 cell line.** Enantioselective toxicity of xenobiotics could be driven by both kinetics (*i.e.*, metabolism and bioaccumulation) and intrinsic toxicity (*i.e.*, protein binding affinity). While we have confirmed that the metabolism of 6PPD-Q contributes to its *in vivo* enantioselective toxicity in rainbow trout, we have not excluded the potential role of intrinsic toxicity. To distinguish between these two confounding factors, *in vitro* fish cell lines would be an ideal model, where the confounding impact of kinetics is excluded. However, to our best knowledge, rainbow trout cell lines have not been benchmarked for 6PPD-Q toxicity testing. Indeed, RTG-2, RTgill-W1 and RTL-W1, three commonly used rainbow trout cell lines, were found insensitive to the toxicity of 6PPD-Q.[24, 30] Therefore, instead of rainbow trout fish cell lines, we decided

to use the coho salmon CSE-119 cell line as it has been recently benchmarked as an *in vitro* model for the toxicity testing of 6PPD-Q.[13, 20] This was further supported by the same toxicity trend of PPD-Qs between CSE-119 cell line and *in vivo* fish testing, confirming that the toxicity pathway was conserved in the CSE-119 cell line.[13]

We then proceeded to test whether the metabolism of 6PPD-Q was active in the CSE-119 cell line. After exposure to (*rac*)-6PPD-Q for 48 hours, only minor amounts (<0.1 % of 6PPD-Q) of $C_4$-OH-6PPD-Q were detected among five OH-6PPD-Qs. This demonstrated that the metabolism of 6PPD-Q was very limited in CSE-119 cells. Consistent with this, similar masses of (*R*)- (0.143 ± 0.04 ng) and (*S*)-6PPD-Q (0.136 ± 0.03 ng, $p = 0.86$) were detected in the same samples of cells (Figure 4A). This further supported that there was no enantioselective accumulation or metabolism of 6PPD-Q in CSE-119 cells. The results validated the CSE-119 cell line as an *in vitro* model for testing the intrinsic toxicity of 6PPD-Q enantiomers, where the contributions of metabolism to enantioselective toxicity can be mitigated as a confounding factor.

We then proceeded to test the toxicity of (*R*)-6PPD-Q and (*S*)-6PPD-Q in the CSE-119 cell line. The $EC_{50}$ of (*R*)-6PPD-Q was determined to be 17.7 µg/L, 3.94 times stronger than that of (*S*)-6PPD-Q (69.7 µg/L) under the same exposure condition (Figure 4B). This demonstrated the enantioselective toxicity of 6PPD-Q, with stronger toxicity observed for (*R*)-6PPD-Q. It should be noted that the stronger toxicity of (*R*)-6PPD-Q in *in vitro* CSE-119 cells was different from the previous *in vivo* study in rainbow trout,[14] where (*S*)-6PPD-Q ($LC_{50}$ = 1.66 µg/L) was more toxic than (*R*)-6PPD-Q ($LC_{50}$ = 4.31 µg/L). This further indicated that the stronger toxicity of (*S*)-6PPD-Q than (*R*)-6PPD-Q in rainbow trout could

be largely attributed to its slower metabolism rate and hence stronger accumulation. However, future studies are warranted to use coho salmon fish to confirm the enantioselective toxicity of 6PPD-Q *in vivo*.

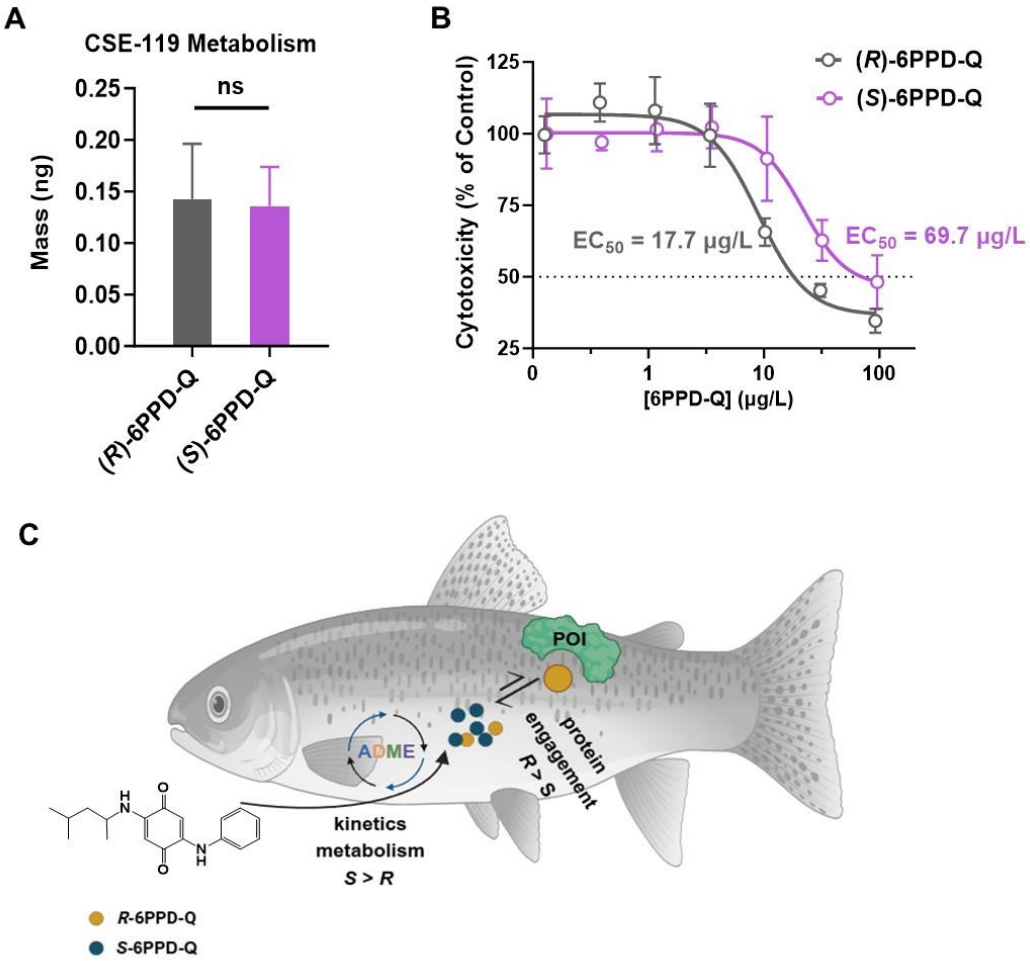


**Figure 4.** Cytotoxicity of 6PPD-Q enantiomers in the coho salmon CSE-119 cell line. (A) The intracellular masses of (*R*)- and (*S*)-6PPD-Q in the CSE-119 cells. (B) The cytotoxicity of (*R*)- and (*S*)-6PPD-Q in the CSE-119 cell line. (C) The schematic figure demonstrates that the kinetics (*e.g.*, metabolism and bioaccumulation) and intrinsic toxicity (*e.g.*, binding to the protein of interest, POI) of 6PPD-Q are both enantioselective.

**Implications.** Previous studies have reported the enantioselective toxicity of 6PPD-Q in rainbow trout, though the mechanism remains unclear.[14, 15] We herein discovered enantioselectivity in both the metabolism and intrinsic toxicity of 6PPD-Q in two sensitive fish species (see the scheme in Figure 4C). The rapid metabolic rate of (*R*)-6PPD-Q leads to its lower *in vivo* toxicity in rainbow trout, which was consistent with our recent finding that hydroxylation of 6PPD-Q was a detoxification process.[22] Notably, enantioselective metabolism of 6PPD-Q was not observed (EF = 0.50 - 0.48) in the artic char (*S. alpinus*) (Figure S7), a species not sensitive to 6PPD-Q. Future studies are warranted to examine whether enantioselective metabolism is fundamentally related to the interspecies variations in toxicity.

Our previous studies suggested that selective protein binding, rather than nonselective toxicity pathways (*e.g.*, reactive oxygenated species, ROS), may mediate the toxicity of 6PPD-Q.[12] This hypothesis was further supported by the enantioselective toxicity of 6PPD-Q in CSE-119 cells, as enantioselectivity is characteristic of protein binding as exemplified by the selective binding of (*S*)-thalidomide to the CRBN protein.[16-18] Taken together, both the kinetics (*e.g.*, metabolism and bioaccumulation) and intrinsic toxicity (*e.g.*, binding to the protein of interest, POI) played important roles in the enantioselective toxicity of 6PPD-Q in salmonids (Figure 4C). However, more comprehensive molecular biology research is needed to identify the metabolic enzyme and POI mediating the metabolism and toxicity of 6PPD-Q.

## Supporting Information Available

The supporting information provides figures addressing: (1) The purification and chiral chromatograms of 6PPD-Q enantiomers; (2) $MS^2$ spectra of hydroxylated metabolites of 6PPD-Q; (3) Chromatograms of $C_4$-OH-6PPD-Q; (4) Metabolism of $C_4$-OH-6PPD-Q in liver S9; (5) EF values of 6PPD-Q enantiomers in the liver S9 of arctic char.

## Author information


### Corresponding authors

**Linna Xie**- Department of Chemistry, University of Toronto, Toronto, Ontario M5S 3H6, Canada;

**Hui Peng** - Department of Chemistry and School of the Environment, University of Toronto, Toronto, Ontario M5S 3H6, Canada;

### Authors

**Rui Li** - Department of Chemistry, University of Toronto, Toronto, Ontario M5S 3H6, Canada;

**Holly Barrett** - Department of Chemistry, University of Toronto, Toronto, Ontario M5S 3H6, Canada;

**Pranav Nair** - Department of Chemistry, University of Toronto, Toronto, Ontario M5S 3H6, Canada;

**Minghua Wang** - Department of Pesticide Science, College of Plant Protection, Nanjing Agricultural University, State & Local Joint Engineering Research Center of Green Pesticide Invention and Application, Nanjing, 210095, China

## Notes

The authors declare no competing financial interests.

## Acknowledgments

This research was supported by National Sciences and Engineering Research Council (NSERC) Discovery Grants and the Great Lakes Fresh Water Ecosystem Initiative (GCXE25A043) from the Environment and Climate Change Canada. The authors acknowledge the support of instrumentation grants from the Canada Foundation for Innovation, the Ontario Research Fund, and the NSERC Research Tools and Instrument Grant. We would like to thank Dr. John D. Hansen and Dr. Justin B. Greer from the U.S. Geological Survey for kindly sharing the CSE-119 cell line.

## References


(1) Klöckner, P.; Seiwert, B.; Wagner, S.; Reemtsma, T., Organic Markers of Tire and Road Wear Particles in Sediments and Soils: Transformation Products of Major Antiozonants as Promising Candidates. *Environ Sci Technol* **2021,** 55 (17), 11723-11732.

(2) Ji, J. W.; Li, C. S.; Zhang, B. J.; Wu, W. J.; Wang, J. L.; Zhu, J. H.; Liu, D. S.; Gao, R. M.; Ma, Y. Q.; Pang, S.; Li, X. F., Exploration of Emerging Environmental Pollutants 6PPD and 6PPDQ in Honey and Fish Samples. *Food Chem* **2022,** 396, 133640.

(3) Rossomme, E.; Hart-Cooper, W. M.; Orts, W. J.; McMahan, C. M.; Head-Gordon, M., Computational Studies of Rubber Ozonation Explain the Effectiveness of 6PPD as an Antidegradant and the Mechanism of Its Quinone Formation. *Environ Sci Technol* **2023,** 57 (13), 5216-5230.

(4) Hu, X. M.; Zhao, H. Q. N. N.; Tian, Z. Y.; Peter, K. T.; Dodd, M. C.; Kolodziej, E. P., Transformation Product Formation upon Heterogeneous Ozonation of the Tire Rubber Antioxidant 6PPD (N-(1,3-dimethylbutyl)-N′-phenyl-p-phenylenediamine). *Environ Sci Technol Let* **2022,** 9 (5), 413-419.

(5) Seiwert, B.; Nihemaiti, M.; Troussier, M.; Weyrauch, S.; Reemtsma, T., Abiotic Oxidative Transformation of 6-PPD and 6-PPD Quinone from Tires and Occurrence of their Products in Snow from Urban Roads and in Municipal Wastewater. *Water Res* **2022,** 212, 118122.

(6) Zhao, H. N.; Hu, X. M.; Tian, Z. Y.; Gonzalez, M.; Rideout, C. A.; Peter, K. T.; Dodd, M. C.; Kolodziej, E. P., Transformation Products of Tire Rubber Antioxidant 6PPD in Heterogeneous Gas-Phase Ozonation: Identification and Environmental Occurrence. *Environ Sci Technol* **2023,** 57 (14), 5621-5632.

(7) Tian, Z.; Zhao, H.; Peter, K. T.; Gonzalez, M.; Wetzel, J.; Wu, C.; Hu, X.; Prat, J.; Mudrock, E.; Hettinger, R.; Cortina, A. E.; Biswas, R. G.; Kock, F. V. C.; Soong, R.; Jenne, A.; Du, B.; Hou, F.; He, H.; Lundeen, R.; Gilbreath, A.; Sutton, R.; Scholz, N. L.; Davis, J. W.; Dodd, M. C.; Simpson, A.; Mcintyre, J. K.; Kolodziej, E. P., A Ubiquitous Tire Rubber-Derived Chemical induces Acute Mortality in *Coho salmon*. *Science* **2022,** 375, 6582.

(8) Tian, Z. Y.; Gonzalez, M.; Rideout, C. A.; Zhao, H. N.; Hu, X. M.; Wetzel, J.; Mudrock, E.; James, C. A.; McIntyre, J. K.; Kolodziej, E. P., 6PPD-Quinone: Revised Toxicity Assessment and Quantification with a Commercial Standard. *Environ Sci Technol Let* **2022,** 9 (2), 140-146.

(9) Brinkmann, M.; Montgomery, D.; Selinger, S.; Miller, J. G. P.; Stock, E.; Alcaraz, A. J.; Challis, J. K.; Weber, L.; Janz, D.; Hecker, M.; Wiseman, S., Acute Toxicity of the Tire Rubber-Derived Chemical 6PPD-Quinone to Four Fishes of Commercial, Cultural, and Ecological Importance. *Environ Sci Technol Let* **2022,** 9 (4), 333-338.

(10) Hiki, K.; Asahina, K.; Kato, K.; Yamagishi, T.; Omagari, R.; Iwasaki, Y.; Watanabe, H.; Yamamoto, H., Acute Toxicity of a Tire Rubber-Derived Chemical, 6PPD Quinone, to Freshwater Fish and Crustacean Species. *Environ Sci Technol Let* **2021,** 8 (9), 779-784.

(11) Hiki, K.; Yamamoto, H., The Tire-Derived Chemical 6PPD-quinone Is Lethally Toxic to the White-Spotted *Char Salvelinus leucomaenis pluvius* but Not to Two Other Salmonid Species. *Environ Sci Technol Let* **2022,** 9 (12), 1050-1055.

(12) Nair, P.; Sun, J.; Xie, L.; Kennedy, L.; Kozakiewicz, D.; Kleywegt, S.; Hao, C.; Byun, H.; Barrett, H.; Baker, J.; Monaghan, J.; Krogh, E.; Song, D.; Peng, H., Synthesis and Toxicity Evaluation of Tire Rubber-Derived Quinones. *ChemRxiv* **2023**.
(13) Xie, L.; Yu, J.; Nair, P.; Sun, J.; Barrett, H.; Meek, O.; Qian, X.; Yang, D.; Kennedy, L.; Kozakiewicz, D.; Hao, C.; Hansen, J. D.; Greer, J. B.; Abbatt, J. P. D.; Peng, H., Structurally Selective Ozonolysis of p-Phenylenediamines and Toxicity in *Coho Salmon* and *Rainbow Trout*. *ChemRxiv* **2024**.
(14) Di, S. S.; Liu, Z. Z.; Zhao, H. Y.; Li, Y.; Qi, P. P.; Wang, Z. W.; Xu, H.; Jin, Y. X.; Wang, X. Q., Chiral perspective evaluations: Enantioselective Hydrolysis of 6PPD and 6PPD-Quinone in Water and Enantioselective Toxicity to *Gobiocypris rarus* and *Oncorhynchus mykiss*. *Environ Int* **2022,** 166, 107374.
(15) Di, S. S.; Xu, H. G.; Yu, Y. D.; Qi, P. P.; Wang, Z. W.; Liu, Z. Z.; Zhao, H. Y.; Jin, Y. X.; Wang, X. Q., Environmentally Relevant Concentrations of S-6PPD-Quinone Caused More Serious Hepatotoxicity Than *R*-Enantiomer and Racemate in *Oncorhynchus mykiss*. *Environ Sci Technol* **2024,** 58 (40), 17617-17628.
(16) Kira, M.; Shiga, Y.; Nakagawa, K.; Matsumoto, A.; Tokita, K.; Terasawa, Y.; Zhang, K.; Tsutao, K.; Nakanishi, T.; Yoshida, S.; Sato, S.; Shibata, N.; Asahi, T., Chiral Inversion of Thalidomide During Crystal Growth by Sublimation. *Cryst Growth Des* **2024,** 24 (8), 3133-3139.
(17) Blanco, S.; Macario, A.; López, J. C., The Structure of Isolated Thalidomide as Reference for its Chirality-Dependent Biological Activity: A Laser-Ablation Rotational Study. *Phys Chem Chem Phys* **2021,** 23 (24), 13705-13713.
(18) Mori, T.; Ito, T.; Liu, S. J.; Ando, H.; Sakamoto, S.; Yamaguchi, Y.; Tokunaga, E.; Shibata, N.; Handa, H.; Hakoshima, T., Structural Basis of Thalidomide Enantiomer Binding to Cereblon. *Sci Rep-Uk* **2018,** 8, 1294.
(19) Hutt, A. J., Chirality and pharmacokinetics: An Area of Neglected Dimensionality? *Drug Metab Dispos* **2007,** 22 (2-3), 79-112.
(20) Kasprzyk-Hordern, B., Pharmacologically Active Compounds in the Environment and their Chirality. *Chem Soc Rev* **2010,** 39 (11), 4466-4503.
(21) Coelho, M. M.; Fernandes, C.; Remiao, F.; Tiritan, M. E., Enantioselectivity in Drug Pharmacokinetics and Toxicity: Pharmacological Relevance and Analytical Methods. *Molecules* **2021,** 26 (11), 3113.
(22) Nair, P.; Barrett, H.; Tanoto, K.; Xie, L.; Sun, J.; Yang, D.; Yao, H.; Song, D.; Hui, Peng., Structure and Toxicity Characterization of Alkyl Hydroxylated Metabolites of 6PPD-Q. *ChemRxiv* **2024**.
(23) Qi, Y. Q.; Qiu, A. Q.; Wei, X. Y.; Huang, Y. T.; Huang, Q.; Huang, W., Effects of 6PPD-Quinone on Human Liver Cell Lines as Revealed with Cell Viability Assay and Metabolomics Analysis. *Toxics* **2024,** 12 (6), 389.
(24) Greer, J. B.; Dalsky, E. M.; Lane, R. F.; Hansen, J. D., Establishing an In Vitro Model to Assess the Toxicity of 6PPD-Quinone and Other Tire Wear Transformation Products. *Environ Sci Technol Let* **2023,** 10 (6), 533-537.
(25) Li, R.; Wu, Y. Y.; Wen, N. H.; Wei, W. J.; Zhao, W.; Li, Y. H.; Zhou, L. L.; Wang, M. H., Assessing Environmental and Human Health Risks: Insight from the Enantioselective Metabolism and Degradation of Fenpropidin. *Environ Pollut* **2024,** 355, 124214.

(26) Zhang, Y. Q.; Li, R.; Tan, Y. T.; Chen, Z. H.; Sang, N. N.; Wang, Z.; Wang, M. H.; Shi, H. Y., A Novel Enantioseparation and Trace Determination of Chiral Herbicide Flurtamone Using UPLC-MS/MS in Various Food and Environmental Matrices Based on Box-Behnken Design. *Food Anal Method* **2022,** 15 (12), 3523-3534.
(27) Zhuoyuan Li , L. X., Pranav Nair ,Juan Tao ,Kyoshiro Hiki ,Chunyan Hao ,Hui Peng, A Colorimetric Method for Naked-eye Detection of 6PPD in Rubber Products and Wastes. *ChemRxiv* **2023**.
(28) Bruhn, T.; Schaumlöffel, A.; Hemberger, Y.; Bringmann, G., SpecDis: Quantifying the Comparison of Calculated and Experimental Electronic Circular Dichroism Spectra. *Chirality* **2013,** 25 (4), 243-249.
(29) Tust, M.; Kohler, M.; Lagojda, A.; Lamshoeft, M., Comparison of the *in vitro* assays to investigate the hepatic metabolism of seven pesticides in *Cyprinus carpio* and *Oncorhynchus mykiss*. *Chemosphere* **2021,** *277*, 130254.
(30) Mahoney, H.; da Silva Junior, F. C.; Roberts, C.; Schultz, M.; Ji, X.; Alcaraz, A. J.; Montgomery, D.; Selinger, S.; Challis, J. K.; Giesy, J. P.; Weber, L.; Janz, D.; Wiseman, S.; Hecker, M.; Brinkmann, M., Exposure to the Tire Rubber-Derived Contaminant 6PPD-Quinone Causes Mitochondrial Dysfunction *In Vitro*. *Environ Sci Technol Let* **2022,** 9 (9), 765-771.

579 **TOC**

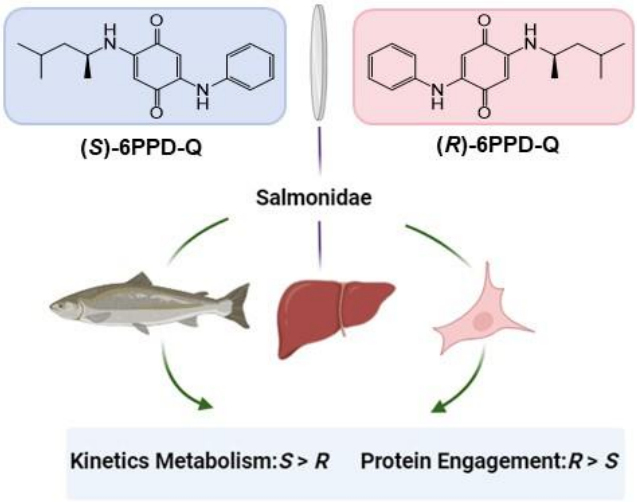


580

581

582